Polar Destabilization of DNA Duplexes with Single-Stranded Overhangs by the *Deinococcus radiodurans* SSB Protein†

Julie M. Eggington,‡ Alexander G. Kozlov,§ Michael M. Cox,*,‡ and Timothy M. Lohman§

Department of Biochemistry, University of Wisconsin−Madison, 433 Babcock Drive, Madison, Wisconsin 53706-1544, and Department of Biochemistry and Molecular Biophysics, Washington University School of Medicine, 660 South Euclid Avenue, St. Louis, Missouri 63110

Received June 13, 2006; Revised Manuscript Received September 14, 2006

ABSTRACT: The *Deinococcus radiodurans* SSB protein has an occluded site size of 50 ± 2 nucleotides on ssDNA but can form a stable complex with a 26−30-nucleotide oligodeoxynucleotide using a subset of its four ssDNA binding domains. Quantitative estimates of *D. radiodurans* SSB protein in the *D. radiodurans* cell indicate approximately 2500−3000 dimers/cell, independent of the level of irradiation. At biologically relevant concentrations, when bound at single-strand−double-strand DNA junctions in vitro, *D. radiodurans* SSB protein has a limited capacity to displace the shorter strand of the duplex, permitting it to bind to single-strand extensions shorter than 26−30 nucleotides. The capacity to displace the shorter strand of the duplex shows a pronounced bias for extensions with a free 3′ end. The *Escherichia coli* SSB protein has a similar but somewhat less robust capacity to displace a DNA strand annealed adjacent to a single-strand extension. These activities are likely to be relevant to the action of bacterial SSB proteins in double-strand break repair, acting at the frayed ends created by ionizing radiation.

Deinococcus radiodurans is of particular interest in DNA repair investigation as it is one of the most radiation resistant organisms known (*1*, *2*). *D. radiodurans* is a soil bacterium featuring a D_{37} γ irradiation dose of approximately 6000 Gy, making this organism roughly 200 times more resistant to radiation than *Escherichia coli* (*1*, *2*). DNA damage is not prevented in *D. radiodurans*. A 6000 Gy dose introduces approximately 300 DNA double-strand (ds) breaks, more than 3000 single-strand (ss) breaks, and more than 1000 sites of base damage per *D. radiodurans* haploid genome (refs *1* and *2* and references therein). *D. radiodurans* repairs its genome with a robust DNA damage repair system. As single-stranded DNA-binding (SSB) proteins are essential to DNA replication, recombination, and repair in all known organisms (*3*), we have pursued the study of *D. radiodurans* SSB (DrSSB) in hopes of shedding greater light on the DNA damage repair system of *D. radiodurans*. The DrSSB protein is unusual among bacterial SSB proteins, having two subunits (each with two OB folds) in place of the much more common four subunits (each with one OB fold) (*4*, *5*). Does this unusual structure play a role in the reconstitution of the *Deinococcus* genome after irradiation?

Bacterial SSB proteins were initially called DNA-unwinding proteins, helix-destabilizing proteins, and other related terms (*6*). However, the primary focus of SSB protein studies in recent years has been on its single-stranded DNA protection and stabilization characteristics, and the emerging interest in cellular protein−SSB protein interactions (*6*−*18*). The traditional helix-destabilizing characteristics of SSB proteins are occasionally still tested in the characterization of newly purified SSB proteins in the form of DNA melting temperature depression assays (*19*, *20*). However, these experiments are designed to measure the efficacy of the SSB protein in binding ssDNA that is transiently exposed when long strands of dsDNA breathe, forming ssDNA bubbles, rather than focusing on the effects of SSB that is initiated at ssDNA overhangs. It is important to consider the effects that SSB proteins have at ssDNA−dsDNA junctions with short and longer ssDNA overhangs, as these DNA structures are common intermediates in many DNA metabolic processes and the expected products of DNA breakage caused by ionizing radiation.

We show in this report that *D. radiodurans* SSB (DrSSB) facilitates a local denaturation of the DNA helix at the ss−dsDNA junction of partially duplex DNAs with overhangs of both 15 and 30 nucleotides. The denaturation occurs with a strong bias favoring 3′ overhangs. We also show that sequential binding of a second DrSSB protein dimer on longer 60-nucleotide overhangs can also destabilize the DNA helix at the ss−dsDNA junction of partial duplexes. We consider these results to be physiologically relevant as care was taken to include both monovalent and divalent cations, known DNA helix stabilizers, in the experimental design. Additionally, quantitation of DrSSB protein in the *D. radiodurans* cell shows that the concentration of DrSSB protein in the cell is more than sufficient for duplex destabilization at ss−dsDNA junctions.

EXPERIMENTAL PROCEDURES

Proteins. The *D. radiodurans* (Dr) and *E. coli* (Ec) SSB proteins were purified as described previously (*5*, *21*).

† This work was supported by grants from the National Institutes of General Medical Sciences to M.M.C. (GM067085) and T.M.L. (GM030498).

‡ University of Wisconsin−Madison.

§ Washington University School of Medicine.

10.1021/bi061178m CCC: $33.50
Published on Web 11/09/2006

Table 1: Oligodeoxyribonucleotides

Oligodeoxyribonucleotides				
Name	Length	Substrate sequence 5' – 3'	Duplex structures	
GAP1	32	*GGTCATTTTTGCGGATGGCTTAGAGCTTAATT		
GAP1comp	32	AATTAAGCTCTAAGCCATCCGCAAAAATGACC	GAP1comp + GAP1	32bp blunt ends
5GAP1	47	GTACTCCTTGCAGACAATTAAGCTCTAAGCCATCCGCAAAAATGACC	5GAP1 + GAP1	32bp 15nt 5′-overhang
3GAP1	47	AATTAAGCTCTAAGCCATCCGCAAAAATGACCGTACTCCTTGCAGAC	3GAP1 + GAP1	32bp 15nt 3′-overhang
J	11	*ACTAATGCTAG		
J2	15	*TTATACTAATGCTAG		
Ts3	20	*TCACTGTTTATACCTCAAGA		
A14	26	*TTCAACAAAGTAAGCAAAATTTAACC		
G1	30	*CGGAAATACTTCGTTCATATTTATTTGTAT		
5D	12	*TGATTACGTGGT		
3D	12	*TGGTGCATTAGT		
3E-12	12	ACTAATGCACCA	3E12 + 3D	12bp blunt ends
5E-27	27	GTACTCCTTGCAGACACCACGTAATCA	5E-27 + 5D	12bp 15nt 5′-overhang
3E-27	27	ACTAATGCACCAGTACTCCTTGCAGAC	3E-27 + 3D	12bp 15nt 3′-overhang
5E-42	42	GTACTCCTTGCAGACACCACGTAATCAGACACCACGTAATCA	5E-42 + 5D	12bp 30nt 5′-overhang
3E-42	42	ACTAATGCACCAGTACTCCTTGCAGACGACCGTATTTACCAT	3E-42 + 3D	12bp 30nt 3′-overhang
5E-57	57	GTACTCCTTGCAGACGACCGTATTTACCATTTCTCAGTAGACTCAACCACGTAATCA	5E-57 + 5D	12bp 45nt 5′-overhang
3E-57	57	ACTAATGCACCAGTACTCCTTGCAGACGACCGTATTTACCATTTCTCAGTAGACTCA	3E-57 + 3D	12bp 45nt 3′-overhang
5E-72	72	GTACTCCTTGCAGACGACCGTATTTACCATTT…(continued on next line)		
		…CTCAGTAGACTCATTCTCAGTAGACTCAACCACGTAATCA	5E-72 + 5D	12bp 60nt 5′-overhang
3E-72	72	ACTAATGCACCAGTACTCCTTGCAGACGACCG…(continued on next line)		
		…TATTTACCATTTCTCAGTAGACTCATTCTCAGTAGACTCA	3E-72 + 3D	12bp 60nt 3′-overhang

Concentrations of DrSSB and EcSSB proteins were determined by absorbance measurements at 280 nm using extinction coefficients of 4.1×10^4 (*5*) and 2.83×10^4 M^{-1} cm^{-1} (*22*).

Oligodeoxynucleotides for Gel Shift and Displacement Assays and for Equilibrium Fluorescence Titrations. Synthetic oligodeoxynucleotides were obtained in PAGE-purified form from Integrated DNA Technologies, Inc. (Coralville, IA). The oligodeoxynucleotides used as binding substrates are listed in Table 1, along with the annealed pairs. The 5′ ends of the radiolabeled DNA, indicated with an asterisk in Table 1, were labeled with γ-^{32}P purchased from Amersham, and T4 polynucleotide kinase purchased from Promega. The manufacturer's recommendations were followed for the radiolabeling. The annealing of DNA duplexes was performed by adding equimolar oligodeoxynucleotides, at a final concentration of 0.5 μM molecules each, to an annealing buffer containing: 20 mM Tris-HCl (pH 8), 40 mM NaCl, and 10 mM $MgCl_2$. The annealing mixture was heated to 95 °C for 5 min, then allowed to slowly cool to room temperature overnight, and then further cooled to 5 °C over 4 h. The duplexes were then stored at −20 °C until they were used, at which time they were thawed on ice. Duplexes with melting temperatures below or close to room temperature were handled only in the cold room at 5 °C. Duplexes were not purified from unannealed oligodeoxynucleotides.

The oligodeoxynucleotides $(dT)_{45}$, $(dT)_{50}$, and $(dT)_{55}$ used in fluorescence equilibrium titration experiments were synthesized using an ABI model 391 automated DNA synthesizer (Applied Biosystems, Foster City, CA) with phosphoramidites from Glenn Research (Sterling, VA). These were further purified to >99% homogeneity by polyacrylamide gel electrophoresis (PAGE) and electroelution as described previously (*23*). Poly(dT) was purchased from Midland Certified Reagent Co. (Midland, TX). Oligodeoxythymidylates and poly(dT) concentrations were determined spectrophotometrically in 10 mM Tris (pH 8.1) and 0.1 M NaCl using an extinction coefficient (ϵ) of 8.1×10^3 M^{-1} (nucleotide) cm^{-1} (*24*). ssDNA (as well as DrSSB) protein samples were dialyzed extensively versus the indicated buffers for use in the titration experiments.

Electrophoretic Mobility Shift Assay on 32 bp Duplex Substrates. The DNA substrates designed to mimic DNA double-strand breaks were 32 bp long and possessed blunt ends, a 5′ 15-nucleotide overhang, and a 3′ 15-nucleotide overhang. These duplexes were GAP1comp + GAP1, 5GAP1 + GAP1, and 3GAP1 + GAP1, respectively (Table 1). GAP1 was 5′ radiolabeled in all cases. Electrophoretic mobility shift assays were used to determine if DrSSB protein could bind to these DNA molecules. DrSSB protein at a final dimer concentration of 0, 50, or 833 nM was incubated with the DNA substrates for 15 min at 30 °C. The reaction conditions were 1.25 nM DNA duplex (if 100% annealing had occurred) or 1.25 nM oligodeoxynucleotide as indicated, 20 mM Tris-HCl (pH 8.0), 0.1 mM EDTA, 100 mM NaCl, 1 mM DTT, 3 mM magnesium acetate, and 10% (w/v) glycerol. The total reaction volume was 20 μL, and 4 μL of 6× loading buffer [18% (w/v) ficoll, 20 mM Tris-acetate (80% cation), and 0.25% (w/v) xylene cyanol] was added to the individual reaction mixtures following the incubation. An aliquot (12 μL) of the resulting reaction volume was loaded onto the gel. A 10% native polyacrylamide gel (1× TBE) was employed and was run at 10 V/cm in the 5 °C cold room for 150 min. Following electrophoresis, the gel was dried for 1 h under vacuum at 80 °C and then exposed to a phosphor-imager screen before scanning. Care was taken to avoid overexposure of the phosphor-imager screen. The screen was scanned with a Typhoon 9410 variable mode imager.

Determination of the Minimal ssDNA Length for DrSSB. The minimal length of a single-stranded oligodeoxynucleotide that could be bound by DrSSB protein was determined by an electrophoretic mobility shift assay in a 9% native polyacrylamide gel (1× TBE). Radioactively labeled oligodeoxynucleotides of 11, 15, 20, 26, and 30 nucleotides (oligodeoxynucleotides J, J2, Ts3, A14, and G1, respectively, in Table 1) were tested at a final molecule concentration of 2 nM. The reaction mixtures contained 0, 25, or 125 nM DrSSB protein dimers. Final buffer conditions were 20 mM Tris-HCl (pH 8), 0.1 mM EDTA, 100 mM NaCl, 1 mM DTT, and 10% glycerol. The reaction mixtures were mixed in tubes kept on ice in a final volume of 20 μL. The reaction

mixtures were then incubated for 5 min at 30 °C. Following incubation, 1.5 μL of 6× loading buffer was added, and the entire reaction volume was loaded onto the gel. The protein−DNA complexes were resolved in the gel at 10 V/cm for 150 min at room temperature in 1× TBE. Following electrophoresis, the gel was dried and exposed to a phosphor-imager screen overnight before being scanned as described.

Oligodeoxynucleotide Displacement Assay. The oligodeoxynucleotide displacement assays for the 12 bp duplexes containing varying lengths of single-stranded DNA were performed in a fashion similar to those of other electrophoretic mobility shift assays described. However, as shown in this report, the radiolabeled 12-nucleotide ss oligodeoxynucleotide is not stably bound by DrSSB protein. The release of the radiolabeled 12-nucleotide ss oligodeoxynucleotide from its annealed pairing partner could therefore be easily monitored in the gel. Duplexes were incubated with different concentrations of DrSSB protein, from 0 to 300 nM DrSSB protein dimers as indicated. EcSSB protein tetramers in the same concentration range were also incubated under these conditions with some of the substrates, as indicated. The reaction mixtures consisted of 1.25 nM duplex DNA (calculated as if 100% annealing had occurred), 20 mM Tris-HCl (pH 8.0), 0.1 mM EDTA, 100 mM NaCl, 1 mM DTT, 3 mM magnesium acetate, and 10% (w/v) glycerol in a total reaction volume of 20 μL. Following a 15 min incubation at 10 °C, 4 μL of 6× loading buffer was added to the individual reaction mixtures, and 12 μL of the resulting reaction volume was loaded onto the gels. All preparations and electrophoresis runs (10 V/cm for 160 min) were performed using 12% native polyacrylamide gels in a 5 °C cold room. Following electrophoresis, the gel was dried and then exposed to a phosphor-imager screen and scanned as described. A Typhoon 9410 variable mode imager was employed for scanning, and TotalLab version 1.10 from Phoretix was used for quantitation.

For the 5E-27 + 5D and 3E-27 + 3D duplexes, corresponding to the 12 bp and 15-nucleotide overhang substrates, the intensities of the remaining duplex bands and the displaced labeled 12-nucleotide oligonucleotide band in each lane were quantitated, and the data were adjusted by subtracting out the intensity due to the initial unannealed portion of the substrate as measured in the lane without protein (*25*). That is, the fraction of displaced ssDNA was calculated as [(% labeled single-strand) − (% labeled single-strand in background)]/[(% total labeled duplex + % labeled single-strand) − (% labeled single-strand background)]. Three to four independent assays were performed to obtain averages and uncertainties.

The quantitation data were not adjusted in the assays using the 12 bp and 30-, 45-, or 60-nucleotide overhang substrates formed from 5E-42 + 5D, 3E-42 + 3D, 5E-57 + 5D, 3E-57 + 3D, 3E-72 + 3D, and 5E-72 + 5D oligodeoxynucleotides (Table 1). For these assays, the major species that can be identified within the gels were quantitated as a percentage of the total counts within the lane and are reported in this format. The quantitation data were not adjusted as described for the shorter 15-nucleotide extensions as protein-bound duplex species were also detected for the longer DNA substrates, complicating the previously used adjustment. For the 45-nucleotide overhang substrates and for the 60-nucleotide overhang substrate, a 1000-fold excess of the corresponding unlabeled 12-mer oligonucleotide was included in the reaction mixture. This allowed for more accurate quantitation of results via experimental separation of the DrSSB displacement effect from the DrSSB annealing stimulatory effect, which became troublesome with these longer substrates (see Results). Three to four independent experiments were performed to obtain averages and uncertainties.

Equilibrium Fluorescence Titrations. Equilibrium binding of DrSSB protein to oligodeoxynucleotides, $(dT)_N$, and poly(dT) was performed by monitoring the quenching of DrSSB protein Trp fluorescence upon addition of ssDNA using a PTI QM-2000 spectrofluorometer (Photon Technologies, Inc., Lawrenceville, NJ) [λ_{ex} = 296 nm (2 nm excitation band-pass) and λ_{em} = 345 nm (2−4 nm emission band-pass)] as described previously (*26*, *27*). The data shown in Figure 4 were analyzed assuming the sequential binding of two $(dT)_{25}$ molecules (*D*) to two sites on the DrSSB protein dimer (*P*) according to eq 1

$$Q = \frac{Q_1 2k_1 D + Q_2 k_1 k_2 D^2}{1 + 2k_1 D + k_1 k_2 D^2} \quad (1)$$

where *Q* is the observed fluorescence quenching, k_1 and k_2 are the stepwise microscopic constants for the binding of the first and second molecules of $(dT)_{25}$ to DrSSB protein, respectively, Q_1 and Q_2 are the values of the maximum quenching associated with one and two bound DNA molecules, respectively, and *D* is the concentration of free ssDNA, which can be obtained from eq 2.

$$D = D_{tot} - D_{bound} = D_{tot} - P_{tot}\frac{2k_1 D + 2k_1 k_2 D^2}{1 + 2k_1 D + k_1 k_2 D^2} \quad (2)$$

The binding isotherms shown in Figure 4 were fit to eqs 1 and 2 using the nonlinear regression package in Scientist (MicroMath Scientist Software, Salt Lake City, UT).

DrSSB Quantitative Western Blots. D. radiodurans Unirradiated and Irradiated Extract Preparation

D. radiodurans culture growth, microscopy, and irradiation were performed as described previously with minor changes (*28*). *D. radiodurans* cultures were grown in TGY broth at 30 °C and harvested in early to mid log phase (OD_{600} = 0.40−0.75 by end of harvest) at 4200*g* for 45 min and then resuspended in magnesium sulfate buffer [10 mM $MgSO_4$ and 10 mM Tris-HCl (pH 7.5)]. Small samples of the homogeneous cell resuspension were removed at this point for dilution plating and for microscopy inspection. The remaining cell resuspension was divided into 10 mL aliquots and pelleted at 8000*g* for 10 min. The clarified magnesium sulfate buffer was removed, and the individual cell pellets were weighed to confirm the equal mass of each pellet. Half of the cells were irradiated with a dose of 3000 Gy over 250 min, while the other half were kept at room temperature for 250 min. Cells were irradiated with a model 484R ^{60}Co irradiator (J. L. Sheppard & Associates, San Fernando, CA). Following irradiation, all cell pellets were stored at −80 °C overnight. Cells were thawed and resuspended in equal volumes of buffer A [50 mM Tris-HCl (pH 6.8), 2 mM EDTA, 2% (w/v) SDS, 1 mM DTT, 10% (w/v) glycerol,

100 mM NaCl, and 1 mM PMSF] to a total of 15 mL. Cell resuspensions were passed twice through a French press (16 000 psi) at room temperature. Cracked cell solutions were then heated to 80 °C for 10 min to denature proteins and then clarified by centrifugation at 14460*g* for 30 min. The clarified solution was recovered, aliquoted into 0.5 mL aliquots, and stored at −80 °C. Total protein concentrations in unirradiated and irradiated *D. radiodurans* clarified cell lysates were determined using the BCA assay (Pierce Chemical, Rockford, IL) with bovine serum albumin as the standard.

Determination of Cell Concentrations. The cell concentration of the samples was calculated by determining the number of colony-forming units (cfu) of the sample, and the percentage of tetracocci and diplococci *D. radiodurans* in each cfu. The concentration of cells in a sample therefore equals [4(tetracocci fraction × cfu) + 2(diplococci fraction × cfu)]/(volume of sample). The homogeneous cell resuspension, removed prior to pellet formation for irradiation, was serially diluted (1:10) in magnesium sulfate buffer and plated on TGY agar plates. Plates were incubated for 2 days at 30 °C, and cfus were counted. The other sample of the homogeneous cell resuspension was fixed for microscopy inspection to determine the number of cells per cfu. Cells were fixed by heating the sample to 80 °C for 20 min and allowed to cool to room temperature, followed by the addition of toluene to a concentration of 1% (v/v) and temporary storage at 4 °C. The fixed samples were later stained with a lipid membrane stain, *N*-(3-triethylammoniumpropyl)-4-{6-[4-(diethylamino)phenyl]hexatrienyl}-pyridinium dibromide (FM 4−64) at a final concentration of 0.011 μg/μL. The cell solution was mounted on glass slides coated with 0.5% agarose. The cells were visualized using a Leica DMRXA2 microscope and the Leica Microsystems N2.1 filter cube containing a 580 nm long-pass dichroic mirror, a 515−569 nm band-pass excitation filter, and a 590 nm long-pass emission filter. Slidebook 4.0 from Intelligent Imaging Innovations, Inc. (Denver, CO), aided in the sample visualization. A sample size of 800 cfus was manually counted and visually determined to be either tetracocci or diplococci.

Electrophoresis and Electrotransfer. Quantitative Western blots were designed for DrSSB protein based upon the method described in ref *29* and optimized for efficient electrotransfer and membrane retention (*30*, *31*). Known amounts of purified DrSSB protein were used as standards, while 50 and 25 μg of proteins from unirradiated and irradiated *D. radiodurans* cell extracts were loaded into different lanes for SDS−PAGE. DdrA, a protein known to be involved in irradiation damage repair and to be upregulated transcriptionally upon irradiation, was used as a positive control for irradiation of the cells (*32*−*34*). DdrA blots required 100 and 50 μg of extract loads for adequate detection. Bio-Rad ReadyGel 10% acrylamide Tris-HCl gels were used for SDS−PAGE and were run for 2 h at 110 V. The manufacturer's recommendations were followed in the use of the Millipore Immobilon-P^{SQ} Transfer Membrane. Transfer buffer consisted of 50 mM Tris, 384 mM glycine, 20% methanol (v/v), and 0.015% SDS (w/v). The transfer was conducted in a Bio-Rad Mini Trans-Blot electrophoretic transfer cell apparatus at 5 °C. Electrotransfer was achieved by applying 30 V for 2 h, 45 V for 1 h, 60 V for 1 h, 80 V for 1 h, and 85 V for 1 h. The amperage rose from 46 mA at 30 V to 400 mA at 85 V. The post-transfer gel was stained with Coomasie Brilliant Blue R 250 to visualize transfer efficiency.

Using Bio-Rad Precision Plus Protein Dual Color Standards transferred from the gel, the >50 kDa section of the membrane was probed for *D. radiodurans* GroEL, the loading control. The 25−50 kDa section of the membrane was probed for DrSSB, and the <25 kDa section of the membrane was probed for DdrA, the radiation exposure positive control. The membrane was blocked with blocking buffer, [0.5% casein (w/v) in Tris-buffered saline (TBS) (pH 7.5)] with 0.03% Tween 20 (v/v).

Immunodetection. All immunodetection steps were performed at room temperature, ∼23 °C. The immunodetection protocol for DrSSB was as follows: incubation for 1 h with a 1:53000 dilution of affinity-purified chicken anti-DrSSB protein polyclonal antibody (Genetel Laboratories, LLC, Madison, WI) in 40 mL of blocking buffer with 0.05% Tween 20, followed by washes in 0.05% Tween 20 phosphate-buffered saline (PBS) (pH 7.4) and then incubation for 1 h with a 1:800000 dilution of affinity-purified rabbit anti-chicken IgY (H&L) horseradish peroxidase (HRP)-conjugated antibody (Genetel Laboratories) in 40 mL of blocking buffer with 0.05% Tween 20, followed by 0.05% Tween 20 PBS washes. The immunodetection protocol for DdrA was as follows: incubation for 90 min with a 1:2000 dilution of affinity-purified chicken anti-DdrA polyclonal antibody (Genetel Laboratories) in 20 mL of blocking buffer with 0.03% Tween 20, followed by short washes in 0.03% Tween 20 PBS and then incubation for 2 h with a 1:400000 dilution of affinity-purified rabbit anti-chicken IgY (H&L) HRP-conjugated antibody in 40 mL of blocking buffer with 0.03% Tween 20, followed by short 0.03% Tween 20 PBS washes. The immunodetection protocol for *D. radiodurans* GroEL was as follows: incubation for 60 min with a 1:40000 dilution of anti-GroEL peroxidase conjugate antiserum (Sigma, St. Louis, MO, product A 8705) in 20 mL of blocking buffer with 0.05% Tween 20, followed by 0.05% Tween 20 PBS washes.

All chemiluminescence detections used Pierce ECL SuperSignal West Dura Extended Duration Substrate and Kodak BioMax Light Film in the final detection step following the manufacturers' recommendations, with film exposure varying from 3 s to 2 min to achieve even exposure and to avoid overexposure. Developed film was digitally scanned, and bands were quantitated using TotalLab version 1.10 from Phoretix. Plots were generated, and regression analysis was performed using Microsoft Excel. Each gel and immunoblot provided two data points from the unirradiated extract and two data points from the irradiated extract. Two separate quantitative Western blot analyses were performed, providing four total data points for each extract.

RESULTS

DrSSB Protein Binds 15-Nucleotide DNA Extensions Adjacent to Duplex DNA. In an effort to examine the interaction of DrSSB protein alone at DNA double-strand breaks, duplex DNAs of 32 bp were designed to mimic double-strand breaks possessing either blunt ends [GAP1comp + GAP1 (Table 1)] or ends with ssDNA overhangs. The

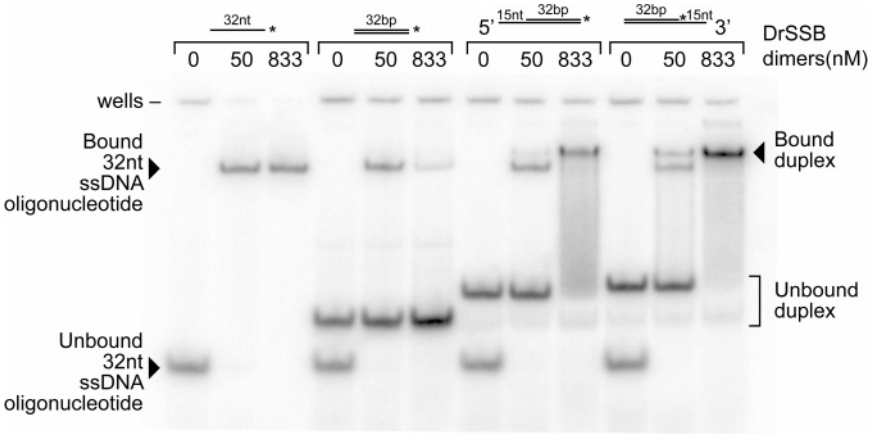

FIGURE 1: Binding of the *D. radiodurans* SSB protein to 32 bp partial duplexes with 15-nucleotide overhangs. Reaction mixtures contained 1.25 nM ^{32}P-labeled oligonucleotide molecules or 1.25 nM DNA duplex or partial duplex (if 100% annealing had occurred) as indicated, 20 mM Tris-HCl (pH 8.0), 0.1 mM EDTA, 100 mM NaCl, 1 mM DTT, 3 mM magnesium acetate, and 10% (w/v) glycerol. The DNA substrates were the labeled 32-nucleotide oligonucleotide alone, the equivalent 32 bp blunt duplex, or the 32 bp duplex with either a 15-nucleotide 5′ ssDNA extension or a 15-nucleotide 3′ ssDNA extension as indicated. The reaction mixture was incubated for 15 min at 30 °C with 0, 50, or 833 nM DrSSB protein dimers. Samples were analyzed on a 10% native polyacrylamide gel as described in Experimental Procedures.

overhang ends consisted of either 5′ or 3′ 15-nucleotide ssDNA [5GAP1 + GAP1 or 3GAP1 + GAP1, respectively (Table 1)]. A 15-nucleotide overhang is within the range of overhang lengths expected for naturally occurring double-strand breaks (*35*). In addition, ends with overhangs are more prevalent than blunt ends in radiation-induced DNA double-strand breaks (*36*). Electrophoretic mobility shift assays (EMSAs) were used to examine the ability of DrSSB protein to bind to these different duplexes.

As seen in the EMSA, DrSSB protein binds efficiently and shifts the unannealed 32-nucleotide ss oligodeoxynucleotide GAP1 as expected (Figure 1). As reported previously for EcSSB (*37*), DrSSB also stimulates the more complete annealing of the unannealed duplex DNA. This effect is most readily seen in the lanes containing the blunt-ended DNA duplexes. Under the buffer conditions that were used, DrSSB protein binds and shifts the 32 bp duplexes possessing either a 5′ or 3′ 15-nucleotide overhang (Figure 1). At 833 nM DrSSB protein dimers, complex formation with the 3′ ss−ds junction appears to have greater stability than complex formation with the 5′ ss−ds junction (Figure 1). Additionally, at a lower concentration of 50 nM DrSSB protein dimer, a higher fraction of DNA is bound by DrSSB protein for the 3′ overhang duplex than for the 5′ overhang DNA duplex substrate. DrSSB protein does not shift the equivalent blunt 32 bp duplex DNA.

As DrSSB protein does not bind the blunt-ended 32 bp duplex but does bind the 15-nucleotide ss−ds DNA junction, this suggests that DrSSB protein is at least binding to the ssDNA overhangs of the overhang double-strand break substrates. The DrSSB protein could either be binding only to the 15-nucleotide ssDNA overhang or be denaturing part of the duplex region exposing more nucleotides for protein binding without completely denaturing the entire duplex. Further experiments were carried out to determine the nature of the DrSSB binding to the ssDNA overhangs.

The Occluded Site Size of the DrSSB Protein Dimer on Poly(dT) Is 50 ± 2 Nucleotides. To investigate the ability of the DrSSB protein to destabilize duplex DNA upon binding to an adjacent single-strand DNA tail, it is important to know the site size of a DrSSB protein−ssDNA complex, defined as the number of nucleotides occluded by the protein, thus preventing a second protein from binding to these nucleotides, upon binding to a long ssDNA. It is expected that the ability to displace the nonoverhang strand of duplex DNA will be minimal if the length of the single-strand overhang is close to the site size.

The occluded site size (n) for binding of the DrSSB protein dimer to poly(dT) has been examined previously (*20*). The reported values depend on solution conditions (mainly salt concentration) and vary from 54 (0.3 M NaCl) to 48 (0.01 M NaCl). It is important to recognize that DrSSB protein−ssDNA binding could occur in different modes, characterized by different site sizes, and that these different modes could be selectively stabilized by different solution conditions. For example, it is well documented that the *E. coli* SSB (EcSSB) protein tetramer, possessing four OB folds, can bind in two principal binding modes which differ in the number of subunits (OB folds) that interact with the ssDNA (*3*). In the $(SSB)_{35}$ mode, stabilized at <20 mM NaCl, two subunits on average interact with the ssDNA, occluding ~35 nucleotides, whereas in the $(SSB)_{65}$ mode, stabilized at >0.2 M NaCl, all four subunits interact with the ssDNA, with the ssDNA wrapping around the SSB protein tetramer (*38*). Although the DrSSB protein is dimeric (*4*, *5*) whereas the EcSSB protein is tetrameric (*39*), both proteins are remarkably similar in their overall structure, and both contain four OB folds, and thus four potential ssDNA binding sites. As a result, the DrSSB protein is likely to also bind to ssDNA using either all or some subset of its OB folds and thus bind to ssDNA in multiple binding modes. Hence, it was important to determine the site size of the DrSSB protein dimer under the conditions used in our EMSA experiments [20 mM Tris (pH 8.0), 0.10 M NaCl, 3 mM magnesium acetate, 1 mM DTT, and 10% (w/v) glycerol], which differ from the solution conditions used in the previous site size determinations (*20*).

The results of equilibrium titrations of the DrSSB protein with poly(dT) under the conditions used in the EMSA experiments are shown in Figure 2A (●). The intrinsic tryptophan fluorescence quenching increases linearly upon

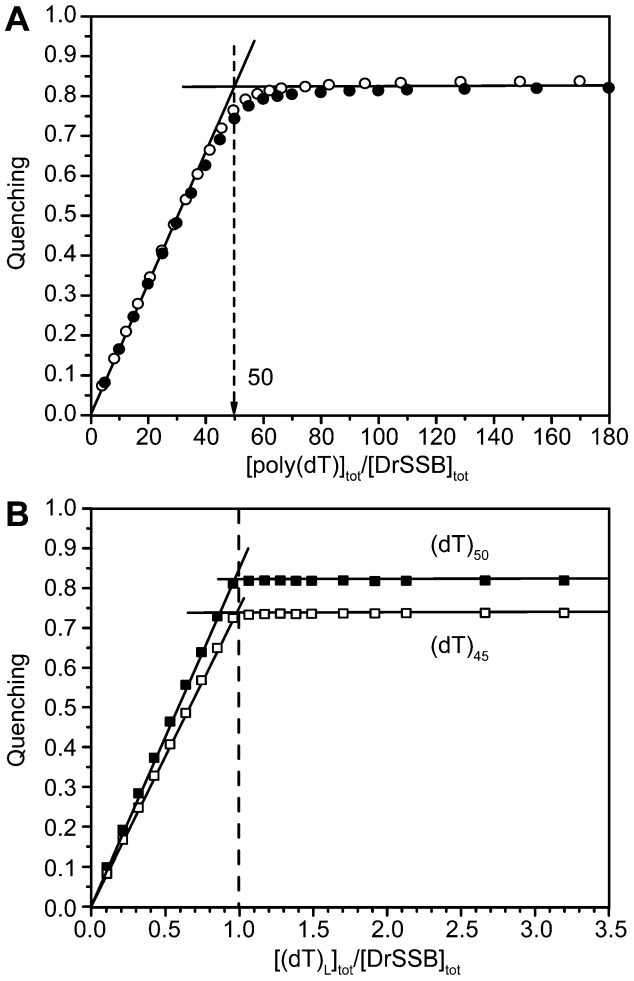

FIGURE 2: Determination of site size of the DrSSB protein dimer using equilibrium fluorescence titrations. (A) "Reverse" titrations of the DrSSB protein dimer with poly(dT) were performed by monitoring intrinsic tryptophan fluorescence quenching ($\lambda_{ex} = 296$ nm; $\lambda_{em} = 345$ nm). The results are plotted as normalized quenching [$Q = (F_0 - F)/F_0$] vs the ratio of poly(dT) (moles of nucleotides) to $[DrSSB]_{tot}$ (moles of dimers): 80 nM DrSSB protein, 20 mM Tris (pH 8.0), 0.1 M NaCl, 3 mM magnesium acetate, 1 mM DTT, and 10% glycerol at 25 °C (●) and 0.2 μM DrSSB protein, 10 mM Tris (pH 8.1), 0.1 mM EDTA, and 0.2 M NaCl at 25 °C (○). An occluded site size (n) of 50 ± 2 was determined from the inflection point as shown on the graph. (B) Titrations of the DrSSB protein (0.2 μM) with 20 μM $(dT)_{45}$ (□) and $(dT)_{50}$ (■) performed in 20 mM Tris (pH 8.0), 0.1 M NaCl, 3 mM magnesium acetate, 1 mM DTT, and 10% glycerol at 25 °C as described for panel A and plotted in a similar manner, except that the $(dT)_L$ concentration is expressed per mole of oligo(dT).

addition of poly(dT) until a plateau value ($Q_{max} \approx 0.83$) is reached, indicating that all protein is bound to poly(dT). The shape of the titration curve indicates that the binding affinity of the DrSSB protein for poly(dT) is very high under these conditions (stoichiometric), so one cannot accurately estimate the equilibrium binding constant but can accurately estimate the occluded site size, which is determined from the inflection point ($n \approx 50 \pm 2$ nucleotides/DrSSB protein dimer). Identical results (○) were obtained in 10 mM Tris (pH 8.1), 0.1 mM EDTA, and 0.2 M NaCl. These values are close to those reported in ref *20* ($Q_{max} = 0.86$; $n = 54$) under their high-salt conditions [0.3 M NaCl, 20 mM phosphate (pH 7.4), and 100 ppm Tween 20].

To further investigate the DrSSB protein site size, we performed fluorescence titrations of the DrSSB protein dimer with a series of oligodeoxythymidylates, $(dT)_L$, varying in length ($L = 45$, 50, and 55 nucleotides). The results obtained under the solution conditions used in the EMSA experiments are shown in Figure 2B. Both $(dT)_{45}$ and $(dT)_{50}$ titrations show linear increases in fluorescence quenching with concentration, indicative of very tight binding (hence, no determination of the binding constant is possible) until a molar ratio of one oligo(dT) per DrSSB protein dimer is reached. Comparison of the $Q_{max,50}$ of ≈0.83 ± 0.2 and the $Q_{max,45}$ of ≈0.76 ± 0.2 with the $Q_{max,poly(dT)}$ of ≈0.83 ± 0.2 suggests that $(dT)_{45}$ is not long enough to interact fully with all of the available ssDNA binding sites on the protein. Identical results were obtained for $(dT)_L$ ($L = 45$, 50, and 55) in 10 mM Tris (pH 8.1), 0.1 mM EDTA, and 0.2 M NaCl (data not shown), although the $Q_{max,55}$ of ≈0.86 ± 0.2 obtained for $(dT)_{55}$ may indicate that the real site size is slightly higher than 50 but is certainly lower than 55.

The Minimal Length of Single-Stranded Oligodeoxynucleotide Bound Stably by the DrSSB Protein Is 26−30 Nucleotides. The occluded site size does not necessarily reflect the minimal oligonucleotide length to which the DrSSB protein dimer can bind. To assess this, we performed EMSA experiments with varying lengths of ss oligodeoxynucleotides using 25 or 125 nM DrSSB protein dimer. As seen in Figure 3, oligodeoxynucleotides with lengths of 11, 15, and 20 nucleotides (J, J2, and Ts3, respectively, in Table 1) are not bound stably by the DrSSB protein in the EMSA experiment. The minimally sized ss oligodeoxynucleotide that can be stably bound in this assay by the DrSSB protein is 26 nucleotides (A14 in Table 1), with a 30-nucleotide oligonucleotide (G1 in Table 1) exhibiting even more stable binding. These results suggest that for the DrSSB protein to bind the 32 bp duplex with a 15-nucleotide extension, some of the duplex region must be melted to expose more ssDNA to form a stable complex with the DrSSB protein.

A DrSSB Protein Dimer Can Bind Two $(dT)_{25}$ Molecules with Apparent Negative Cooperativity. On the basis of the EMSA analysis (see Figure 3), a DrSSB protein dimer is able to form stable complexes with ss oligodeoxynucleotides with lengths of ≥26 nucleotides. Since the occluded site size determined with poly(dT) is ≈50 ± 2 nucleotides, this suggests that one DrSSB protein dimer should be able to bind two ss oligodeoxynucleotides with lengths of 26 nucleotides. We investigated this possibility by performing equilibrium titrations of the DrSSB protein dimer with $(dT)_{25}$ by monitoring quenching of the intrinsic tryptophan fluorescence of the protein upon binding ssDNA. The results of two titrations performed at total DrSSB protein concentrations of 0.14 and 0.5 μM are shown in Figure 4 (10 mM Tris (pH 8.1), 0.1 mM EDTA, and 0.2 M NaCl). As we demonstrated in our poly(dT) experiments (see Figure 2A), under these conditions, the behavior of the protein is identical to that observed under the solution conditions used for our band shift experiments. The biphasic shape of the isotherms shown in Figure 4 clearly indicates that two molecules of $(dT)_{25}$ can bind to one DrSSB protein dimer with the second $(dT)_{25}$ binding with lower affinity. Global nonlinear least-squares fitting of these data to a two-site binding model (eq 1) yields the following parameters: $Q_1 = 0.51 \pm 0.01$ and $k_1 = (1.6 \pm 0.3) \times 10^7\ M^{-1}$ for binding of the first $(dT)_{25}$ molecule and $k_2 = (4.3 \pm 0.6) \times 10^5\ M^{-1}$ for binding of the second $(dT)_{25}$ [for this analysis, the maximum quenching

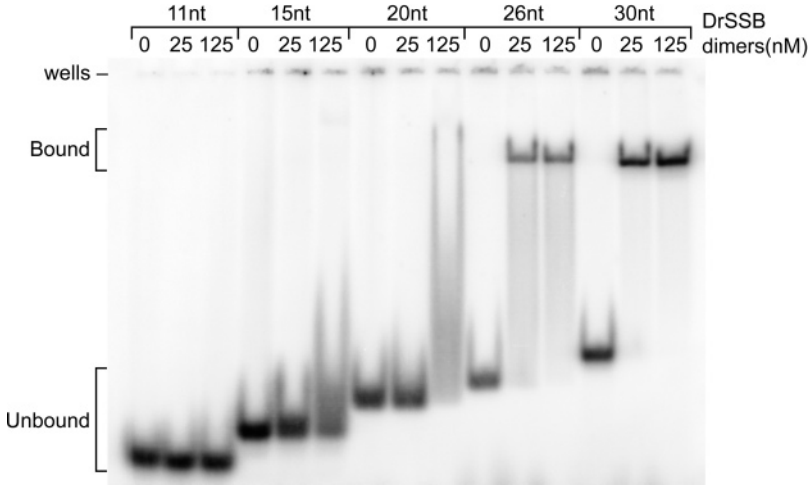

FIGURE 3: Binding of the *D. radiodurans* SSB protein to ssDNA oligonucleotides of increasing size. Reaction mixtures contained 2 nM ^{32}P-labeled oligonucleotide molecules of 11, 15, 20, 26, or 30 nucleotides as indicated, 20 mM Tris-HCl (pH 8.0), 0.1 mM EDTA, 100 mM NaCl, 1 mM DTT, and 10% (w/v) glycerol. The reaction mixture was incubated for 5 min at 30 °C with 0, 25, or 125 nM DrSSB protein dimers. Samples were analyzed on a 9% native polyacrylamide gel as described in Experimental Procedures.

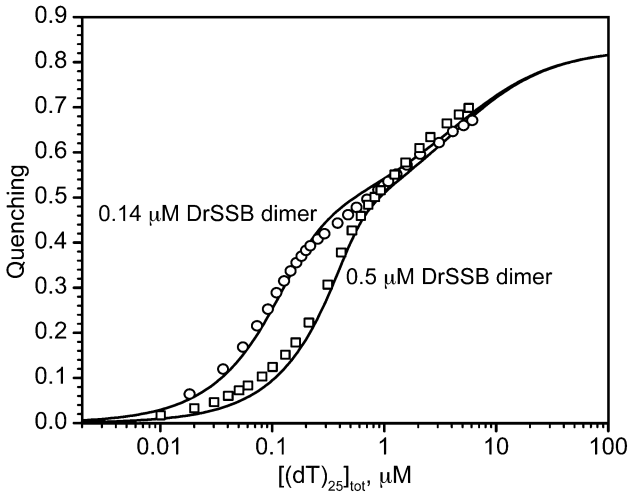

FIGURE 4: DrSSB protein dimer exhibits apparent negative cooperativity upon binding of two $(dT)_{25}$ molecules. Titration of the DrSSB protein [0.14 (○) and 0.5 μM (□)] with $(dT)_{25}$ in 10 mM Tris (pH 8.1), 0.1 mM EDTA, and 0.2 M NaCl at 25 °C. Solid curves represent the results of global nonlinear least-squares fitting of both sets of data to the two-site model (see Experimental Procedures) with best fit parameters: $Q_1 = 0.51 \pm 0.01$, $k_1 = (1.6 \pm 0.3) \times 10^7$ M^{-1}, and $k_2 = (4.3 \pm 0.6) \times 10^5$ M^{-1} [the value of Q_2 of 0.83 was fixed according to the maximum quenching observed in poly(dT) experiments].

upon binding both $(dT)_{25}$ molecules, Q_2, was fixed at 0.83 on the basis of the maximum quenching observed in the poly(dT) experiments]. Therefore, the binding of the second $(dT)_{25}$ molecule occurs with an approximately 40-fold lower microscopic affinity than for the binding of the first $(dT)_{25}$ (i.e., there is apparent negative cooperativity). This implies that binding of the second ssDNA molecule to the DrSSB protein is possible with only a large excess of ssDNA. Since our EMSA experiments are performed under conditions of excess protein over DNA, we exclude the possibility that the ssDNA substrates used in our study can form doubly ligated complexes with one DrSSB protein dimer through their single-stranded overhangs.

DrSSB Protein Denatures Duplex DNA Immediately Adjacent to 15-Nucleotide Single-Stranded Overhangs with a 3′ Overhang Preference. To determine if the DrSSB protein is able to destabilize some part of the duplex DNA immediately adjacent to the ssDNA overhang, we examined the binding of the DrSSB protein to a ss−ds DNA possessing a shorter 12 bp duplex region with a 15-nucleotide overhang. This substrate design was used so that if several base pairs or more were destabilized by the DrSSB protein the shorter labeled 12-nucleotide oligonucleotide would be entirely displaced. The 12 bp duplexes were designed to be comparable to one another in that the duplex sequence at the duplex−ssDNA junction was identical when the 3′ extension duplex is compared to the 5′ extension duplex. That is, these sequences were inverted in the 5′ to 3′ direction with respect to one another. These duplexes are 5E-27 + 5D and 3E-27 + 3D (Table 1).

As seen in the representative gel in Figure 5A, the percentage of total annealed DNA substrate in the starting material was inherently lower for these short 12 bp duplexes than for the longer duplexes used in Figure 1. All oligodeoxynucleotide preparations contained unannealed labeled single-stranded oligodeoxynucleotides, and this unannealed fraction, between 39 and 52% depending on the run (determined in the no protein lane), was subtracted as background as is done in similar unwinding assays for other proteins (*25*). Also, due to the low melting temperature of these 12 bp duplexes, the incubations in these assays were at 10 °C and the gels were run at 5 °C. The radiolabeled 12-mers, 3D and 5D, are too short to be stably bound by the SSB proteins. Therefore, denatured 12-mers run with the unannealed 12-mers. This is taken into account in the quantitations of the EMSA experiments in Figure 5B (for DrSSB protein) and Figure 5C (for EcSSB protein). Experiments with EcSSB protein were also performed for comparison. The percentage of oligodeoxynucleotide displaced was calculated after subtraction of the amount of unannealed 12-mer present in the absence of protein (see Experimental Procedures). Such corrections were not made for the minor fraction of duplexes presumably annealed due to the stimulatory effect of DrSSB as previously noted for the 32 bp duplexes (Figure 1). This slight stimulation of strand annealing was observed with the 12 bp blunt end duplexes (data not shown) that were resistant to denaturation in the

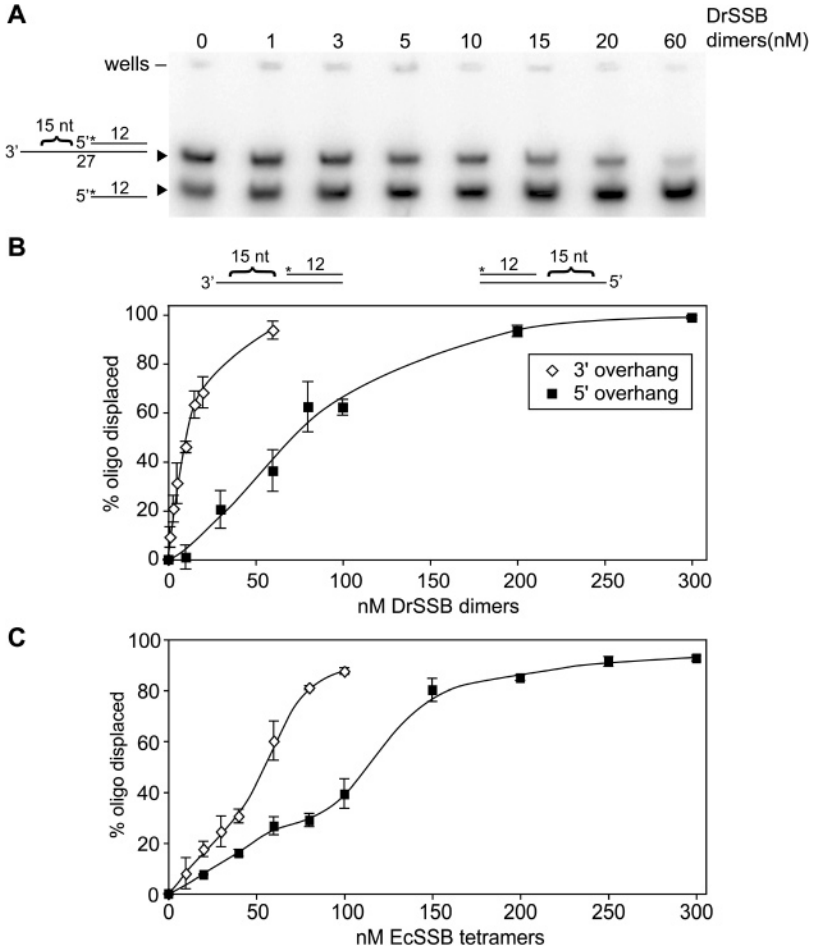

FIGURE 5: Denaturing of short 12 bp DNA partial duplexes with 15-nucleotide overhangs by *D. radiodurans* SSB and *E. coli* SSB proteins at various concentrations. Reaction mixtures contained 1.25 nM ^{32}P-labeled DNA partial duplex (if 100% annealing had occurred), 20 mM Tris-HCl (pH 8.0), 0.1 mM EDTA, 100 mM NaCl, 1 mM DTT, 3 mM magnesium acetate, and 10% (w/v) glycerol. The DNA substrates were the labeled 12 bp partial duplex with either a 15-nucleotide 5′ ssDNA extension or a 15-nucleotide 3′ ssDNA extension as indicated. The reaction mixture was incubated for 15 min at 10 °C with a 0−300 nM range of either DrSSB protein homodimers or EcSSB protein homotetramers as indicated. Samples were analyzed on a 12% native polyacrylamide gel and quantitated as described in Experimental Procedures. (A) A representative gel showing the results of incubation of the DrSSB protein with the 3′ overhang DNA substrate. (B) A plot obtained by band quantitation showing the percentage of labeled 12-nucleotide oligonucleotide displaced at varying concentrations of DrSSB protein homodimers. Empty diamonds represent the results for protein incubation with the 3′ overhang DNA substrate, and filled squares represent the results for incubation with the 5′ overhang DNA substrate. (C) Same as panel B, except with EcSSB protein homotetramers rather than DrSSB protein homodimers.

DrSSB protein dimer concentration range that was tested (up to 300 nM).

As indicated in Figure 5, both DrSSB and EcSSB proteins are able to denature the 12 bp duplexes that possess a 15-nucleotide ssDNA overhang. Interestingly, lower protein concentrations are required for this process when the overhang is a 3′ 15-nucleotide overhang than when it is a 5′ 15-nucleotide overhang. Maximum melting by DrSSB protein of the 3′ overhang substrate is achieved at ∼60 nM dimers, whereas maximum melting of the 5′ overhang substrate is reached at ∼200 nM dimers (Figure 5B). For the EcSSB protein, maximum melting of the 3′ overhang duplex is achieved at ∼100 nM tetramers, while maximum melting of the 5′ overhang duplex is achieved at ∼250 nM tetramers (Figure 5C). Therefore, these proteins both have a preference for melting a duplex possessing a 3′ overhang. However, the DrSSB protein dimers are able to denature both 5′ and 3′ overhang duplexes at slightly lower concentrations than are the EcSSB protein tetramers.

One DrSSB Protein Dimer Can Stably Bind a 45-Nucleotide Overhang without Denaturing the Adjoining Duplex Region. Having found that the DrSSB protein can denature short 12 bp DNA duplexes adjacent to short 15-nucleotide ssDNA overhangs, we tested to see if an overhang length could be found where presumably only one DrSSB protein dimer could bind but not denature the adjoining 12 bp duplex region. To test this, we designed the same 12 bp duplex but with 3′ or 5′ extensions of 30 and 45 nucleotides (Figure 6D−G). The lengths of 30 and 45 nucleotides were chosen as they were intermediate lengths between the occluded site size (50 ± 2 nucleotides under these conditions) and the minimal oligonucleotide length that the DrSSB protein can bind (26−30 nucleotides). EMSA experiments were performed with increasing concentrations of the DrSSB protein, similar to the assays performed with the shorter 15-nucleotide overhangs (see Figure 5).

The plots in Figure 6 show the total radiolabeled species detected in the gels. The major radiolabeled species in the

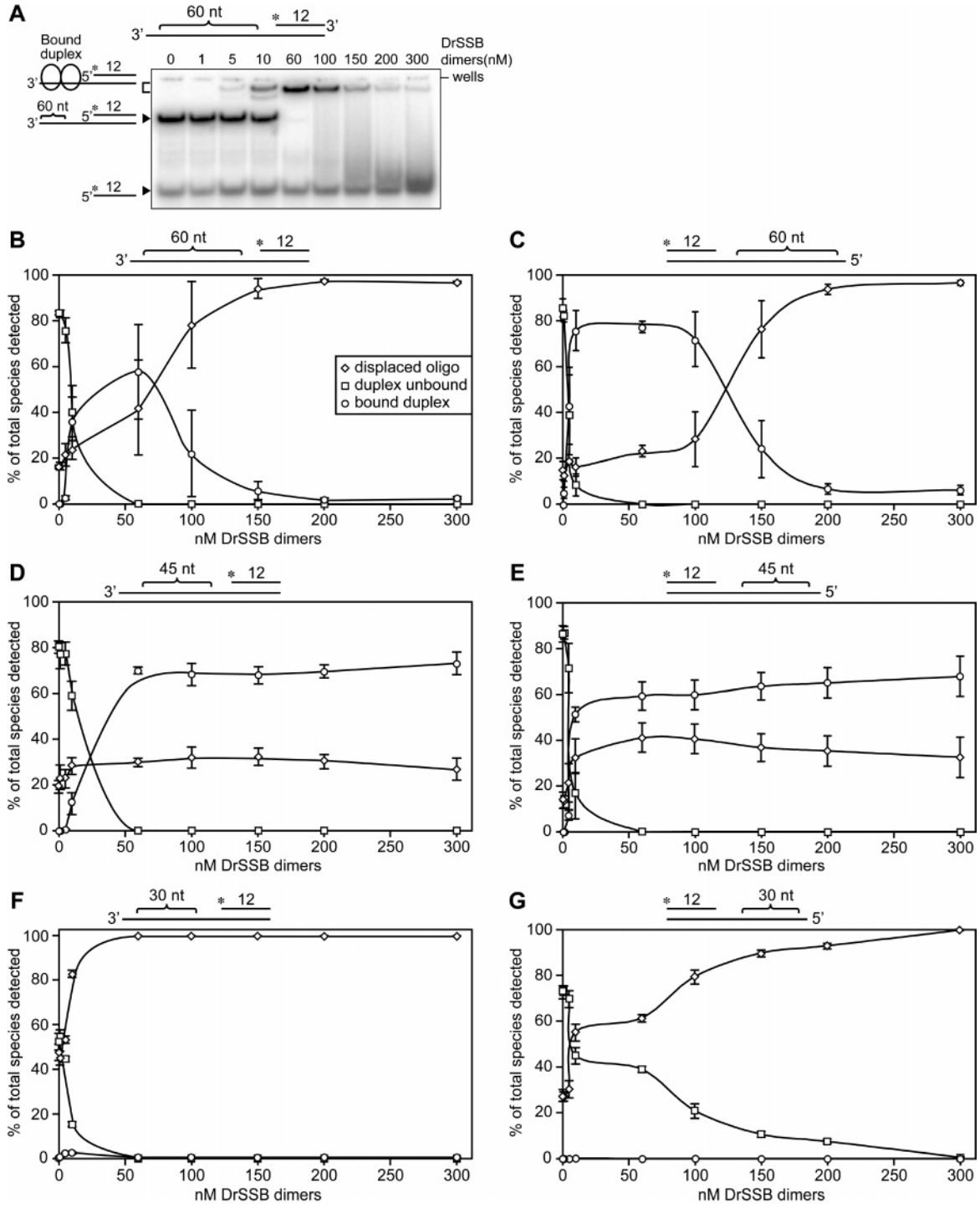

FIGURE 6: Effect of the *D. radiodurans* SSB protein at various concentrations on short 12 bp DNA partial duplexes with 30-, 45-, or 60-nucleotide overhangs. Reaction mixtures contained 1.25 nM ^{32}P-labeled DNA partial duplex (if 100% annealing had occurred), 20 mM Tris-HCl (pH 8.0), 0.1 mM EDTA, 100 mM NaCl, 1 mM DTT, 3 mM magnesium acetate, and 10% (w/v) glycerol. The DNA substrates were the labeled 12 bp partial duplex with either 5′ ssDNA extensions or 3′ ssDNA extensions of varying length as indicated. The reaction mixture was incubated for 15 min at 10 °C with a 0−300 nM range of DrSSB protein homodimers as indicated. Samples were analyzed on a 12% native polyacrylamide gel and quantitated as described in Experimental Procedures. (A) A representative gel showing the results of incubation of the DrSSB protein with the 3′ 60-nucleotide overhang DNA substrate. (B) A plot obtained by band quantitation showing the different species within the gel as a percentage of the total labeled species detected for the 3′ 60-nucleotide overhang DNA substrate. Empty diamonds represent the results for displaced 12-nucleotide oligonucleotide species unbound by protein, empty squares the results for partial duplex species unbound by protein, and empty circles the results for the DrSSB protein-bound partial duplex species. The marker symbols are the same in all subsequent plots. The other panels show plots of the same type with (C) the 5′ 60-nucleotide overhang DNA substrate, (D) the 3′ 45-nucleotide overhang DNA substrate, (E) the 5′ 45-nucleotide overhang DNA substrate, (F) the 3′ 30-nucleotide overhang DNA substrate, and (G) the 5′ 30-nucleotide overhang DNA substrate.

gel were either the displaced radiolabeled 12-mer, unbound ss−ds junction DNA, or DrSSB protein bound to the ss−ds junction DNA. The percentages shown in Figure 6 reflect quantitation of each species without correction for the unannealed fraction of oligodeoxynucleotides that are present in the substrate preparation.

Binding of the DrSSB protein to the shorter 30-nucleotide overhang substrates, 5E-42 + 5D and 3E-42 + 3D, resulted in complete duplex displacement at a concentration of 300 nM DrSSB protein dimer for the 5′ overhang (Figure 6G) and a concentration of 60 nM DrSSB protein dimer for the 3′ overhang (Figure 6F). Hence, the 30-nucleotide overhang and 12 bp duplex DNA substrates showed the same 3′ overhang preference for displacement seen with the 15-nucleotide overhang DNA substrates (see Figure 5). Therefore, 30-nucleotide overhangs were not sufficiently long to provide sufficient ssDNA for DrSSB protein dimer binding without denaturation of the adjacent duplex region.

Longer overhangs of 45 nucleotides, either 3′ (Figure 6D) or 5′ (Figure 6E) to the 12 bp duplex, 3E-57 + 3D or 5E-57, respectively, were of sufficient length for the majority of the DNA substrates to be stably bound by the DrSSB protein without duplex displacement within a DrSSB protein concentration range of up to 300 nM DrSSB protein dimers. However, a fraction (~25−30%) of the duplexes for both the 3′ and 5′ overhang cases were denatured even at lower DrSSB protein concentrations, ≤60 nM DrSSB protein dimers. The fraction of denatured duplexes did not increase with further increases in DrSSB protein concentration past 60 nM. It may be that the fraction of denatured duplexes results from binding of some of the DrSSB protein dimers closer to the duplex region than to the free ssDNA end, and thus, in the process of completing its binding, the DrSSB protein dimer denatures the duplex region. Nevertheless, the majority of the DrSSB protein dimers can bind exclusively to the ssDNA overhang without the need to melt out regions of the duplex DNA.

Again, some stimulation of strand annealing in the unannealed substrate was apparent with the addition of DrSSB protein. As the duplex overhangs are made longer, this stimulation of annealing increased significantly, making quantitation of each species difficult. The stimulation of strand annealing was therefore controlled in the 45-nucleotide overhangs, and later in the 60-nucleotide overhang cases, by challenging with a large excess (1000-fold) of cold 12-mer oligonucleotide, either 3D or 5D, as appropriate. Thus, only the radiolabeled 12-mers that annealed during the substrate preparation were followed in the gel shift assay in these experiments.

Sequential Binding of Multiple DrSSB Protein Dimers on Substrates with Longer Single-Stranded DNA Overhangs Also Results in Denaturation of an Adjoining Duplex DNA. Having found that the DrSSB protein can stably bind a 45-nucleotide extension adjacent to a 12 bp duplex without melting out the adjoining duplex region, we examined the ability of DrSSB protein to denature a 12 bp duplex attached to a longer ssDNA extension. For this purpose, we examined 12 bp duplexes with either a 60-nucleotide 3′ extension or a 60-nucleotide 5′ extension and performed DrSSB protein titrations and EMSA analysis as described above (Figure 6). The 12 bp duplexes with both overhangs were denatured by the DrSSB protein, but at a concentration much higher than that observed for the shorter ssDNA overhangs, suggesting that multiple DrSSB protein dimers were required to melt the duplex regions (see Figure 6B). As with the shorter ssDNA overhangs, there was still a preference for melting of the 12 bp duplexes that possessed 3′ overhangs (cf. panels B and C of Figure 6).

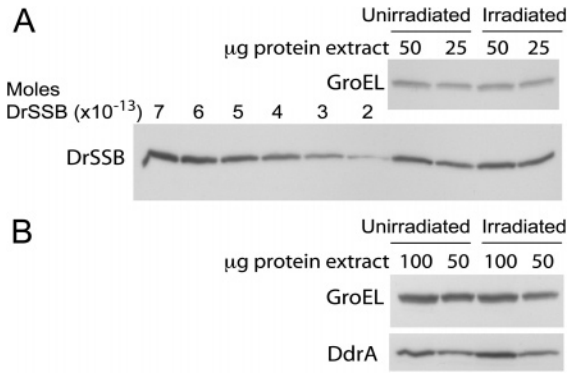

FIGURE 7: *D. radiodurans* SSB protein quantitative Western blot analysis. (A) Representative immunoblot of *D. radiodurans* GroEL and DrSSB proteins from unirradiated and irradiated whole cell extract, 50 and 25 μg of total protein, respectively. GroEL serves as the loading control. Known amounts of pure DrSSB protein are also included in the immunoblot. Note that DdrA was poorly detected at these levels of crude extract. (B) A representative immunoblot of *D. radiodurans* GroEL and DdrA proteins from the same unirradiated and irradiated whole cell extracts as in panel A except with 100 and 50 μg of total protein loads, respectively. DdrA serves as a positive control for upregulation in irradiated cells.

These results suggest that a 60-nucleotide overhang is sufficiently long to allow binding of a single DrSSB protein dimer without the need to invade the duplex region. With an increase in the DrSSB protein concentration, a second DrSSB protein dimer can bind partially to the 60-nucleotide overhang; however, denaturation of the 12 bp duplex is needed to stabilize the binding of the second DrSSB protein dimer. Thus, the sequential binding of DrSSB protein dimers on longer ssDNA overhangs is also able to denature short adjoining duplex regions of DNA.

The DrSSB Protein Dimer Concentration in D. radiodurans Cells Is Approximately 63 μM and Is Not Significantly Upregulated upon Irradiation. Quantitative Western blots were used to determine if the DrSSB protein concentration range used in our in vitro assays is biologically relevant. Panels A and B of Figure 7 show representative immunoblots. The in vitro DrSSB protein dimer concentrations required for duplex melting at ss−dsDNA junctions in our assays were in the range of 10−300 nM DrSSB protein dimers. In vivo DrSSB protein concentrations in this range or higher would suggest that our results are biologically relevant. Quantitation of whole cell protein extracts of unirradiated exponential phase *D. radiodurans* cells showed that these cells contain 2500 ± 800 DrSSB protein dimers per cell ($n = 4$). Extracts from cells immediately following a 3000 Gy dose of ionizing irradiation over 250 min contain ~3000 ± 900 DrSSB protein dimers per cell ($n = 4$). The linear regression analysis of the DrSSB protein standards for the two independent Western blots testing the same extracts gave R^2 values of 0.9656 and 0.9936 (corresponding to the representative immunoblot in Figure 7A). The *D. radiodurans* GroEL loading control bands showed that equal amounts of whole cell protein extract were loaded for the unirradiated and irradiated cell extracts. The positive control, DdrA, required a greater protein load for optimal detection. Extracts used in these detections were identical to those used for DrSSB protein detection. DdrA exhibited a reproducible 1.5-fold increase in the irradiated cell extracts over the unirradiated extract (Figure 7B), showing that these cells had

indeed been irradiated and were responding to the damage (*32*).

Assuming an average cell volume of 6.5×10^{-2} μm^3 (*40*), the quantitations of the DrSSB protein correspond to ~63 ± 21 and ~76 ± 24 μM DrSSB protein dimers in the unirradiated and irradiated cell, respectively. Thus, there is not a significant upregulation of DrSSB protein in the cell during a 250 min course of high-level irradiation. In both the unirradiated and irradiated cell, the DrSSB protein concentration is more than 200-fold higher than what would be needed to facilitate duplex melting in vitro, based on the results reported here. Thus, our in vitro experiments were performed at concentrations that are biologically relevant.

DISCUSSION

The DrSSB protein dimer binds to polymeric ssDNA with an occluded site size of 50 ± 2 nucleotides, presumably in a binding mode so that all four OB folds interact with ssDNA. However, the DrSSB protein is also able to form a stable complex with shorter oligodeoxynucleotides of only 26−30 nucleotides, presumably through interactions using only two OB folds. On a duplex DNA molecule with a ssDNA extension, a single DrSSB protein dimer can also bind to ssDNA extensions that are shorter than the 26−30-nucleotide minimum binding site. However, to do this, DrSSB promotes a strand separation or melting of part of the adjacent duplex region to maximize its interactions up to a total of ~50 nucleotides. This can occur since the binding free energy gained from the additional interactions exceeds the free energy required to melt the duplex. Therefore, DrSSB can displace the shorter strand of a partial duplex when it binds to single-strand extensions of fewer than 30 nucleotides. If the ssDNA extension is greater than or equal to 45−50 nucleotides in length, then displacement of a short duplex requires the binding of a second DrSSB protein dimer. The ability of the DrSSB protein to partially melt a duplex also shows a pronounced bias for extensions with a free 3′ end. The EcSSB protein has a similar but somewhat less robust capacity to displace a DNA strand annealed adjacent to a single-strand extension. Our estimates are that the concentration of the DrSSB protein in *D. radiodurans* cells is at levels well above those needed for the melting of a partial DNA duplex. (We note that the quantitation of the DrSSB protein reported here differs from that mentioned in ref *4* of unpublished preliminary data which overestimated the amount of DrSSB protein in the cell due to a nonoptimized procedure.)

The DrSSB protein, and for comparison the EcSSB protein, both exhibited a capacity to displace short 12 bp duplex DNA adjacent to 15-nucleotide extensions (Figure 5), although the DrSSB protein appeared to be slightly more robust than the EcSSB protein in facilitating the displacement reaction. The EcSSB protein has previously been reported to denature and displace DNA duplexes adjacent to ssDNA extensions, but with no preference for 5′ or 3′ extensions. However, these experiments were not controlled for sequence differences, were performed at a temperature higher than that of the experiments reported here, and were carried out in a buffer containing no added salt (*41*), which would lower the stability of the DNA duplex. These conditions may have masked the 3′ overhang preference of the EcSSB protein.

Since SSB proteins generally have little affinity for duplex DNA, it has been proposed that they facilitate duplex DNA melting by a passive mechanism in which the protein binds to ssDNA that is formed transiently via thermal fluctuations in the duplex DNA (*6*, *42*). Using such a mechanism, a DrSSB protein dimer bound to a ssDNA extension that is shorter than the occluded site size of the protein, but adjacent to a duplex region, should more readily facilitate duplex destabilization since it is poised to capture the transiently formed ssDNA. The crystal structure of the EcSSB protein tetramer bound to ssDNA (*39*) shows that ssDNA binds with a defined orientation with respect to the 3′ to 5′ polarity of the ssDNA. Assuming that ssDNA also binds to the DrSSB protein dimer with a similar defined polarity [which is likely due to the DrSSB protein's many similarities in structure with the EcSSB protein tetramer (*4*)], then the available ssDNA binding sites within the DrSSB protein will be correctly oriented to bind to one of the strands of ssDNA that form transiently at the ss−dsDNA junction.

The displacement experiments reported here were performed in the presence of 100 mM Na^+ and 3 mM Mg^{2+}. These conditions were used on the basis of current estimates of salt concentrations in vivo (*43*, *44*) as well as indications that high divalent cation concentrations exist in the *D. radiodurans* cell (*45*). The passive duplex melting mechanism suggests that the SSB protein should be better able to invade lower-stability duplex regions. Consistent with this idea, we observed more pronounced displacement of duplex regions in buffers that contained no Mg^{2+} (data not shown), the presence of which is known to greatly stabilize duplex DNA (*46*−*48*). A similar inhibition by Mg^{2+} of the ability to destabilize duplex DNA adjacent to a ssDNA region has also been observed for viral SSB proteins (*49*−*51*). Several reports have examined the helix destabilizing properties at ss−dsDNA junctions of the herpes simplex virus type 1 ICP8 protein (*49*), the adenovirus DNA-binding protein (DBP) (*50*, *51*), and the baculovirus LEF-3 protein (*41*). All three of these proteins can destabilize short duplex DNA regions, ranging from 17 bp to at least 200 bp, depending upon the protein and the assay. These duplex regions were attached to ssDNA extensions similar in length or longer than those used in the studies reported here. However, the assays for complete displacement of these duplex regions were performed in buffers containing very low or no added salt; the capacity of these proteins to completely denature the DNA substrates dramatically dropped as the monovalent and divalent cation concentrations were increased to levels approaching those used in our assays (*49*−*51*). Under the low-salt or no-salt conditions used in the viral SSB protein studies, ICP8 and DBP exhibited no polarity effects in their abilities to melt a duplex region (*49*−*51*), whereas LEF-3 exhibited a preference for 5′ single-strand extensions (*41*). However, those experiments were not controlled for sequence equivalence between the DNA substrates that were tested.

Our studies have shown that the sequential binding of DrSSB protein dimers to partial DNA duplexes with 60-nucleotide ssDNA extensions can result in the complete displacement of an adjoining 12 bp duplex (Figure 6). Although DNA double-strand breaks typically do not have such long ssDNA regions (*35*, *36*), collapsed replication forks and other intermediate DNA structures that can form during DNA repair (*52*) will often have a primer−template structure

with longer tracts of exposed ssDNA. Sequential binding of SSB proteins to these exposed regions of ssDNA may not only provide protection and stabilization (*6*) but also partially melt the adjoining duplex region, perhaps providing a needed signal and/or anchoring point.

RPA, the heterotrimeric eukaryotic SSB protein, has very similar binding characteristics at ss−dsDNA junctions (*53*−*56*). When presented with duplex DNAs with short ssDNA extensions, RPA has a marked bias toward the binding of 3′ extensions, much as we report here for the SSB protein (*53*). The results imply a defined polarity of RPA binding, which demonstrably affects the activities of other enzymes that interact with RPA and that are involved in DNA metabolism at single-strand gaps (*53*). RPA has also been shown to recognize DNA primer−template junctions by direct contact with the recessed 3′ end of the priming strand (*55*, *56*). Just as we propose, the primer−template junction interaction by RPA has been suggested as a mechanism for signaling to other proteins the presence of an available DNA synthesis initiation site and for acting as a protein anchor for other proteins (*56*). This type of protein interaction at DNA primer−template junctions could possibly be a general feature of SSB proteins across the biological spectrum. As with RPA, the SSB protein is known to interact with a wide range of proteins in DNA metabolism. The binding polarity of the SSB protein demonstrated here could have functional significance in a similarly wide range of processes.

In summary, the ability of bacterial SSB proteins to partially melt DNA duplex regions attached to ssDNA extensions has not been previously addressed in detail but may be relevant to its function in DNA metabolism. Although we designed our DNA substrates to approximate what might exist at DNA double-strand breaks, we also note that the DNA substrates with 5′ ssDNA extensions also resemble the type of DNA structures present at primer−template junctions during DNA replication. Thus, the overall finding that DrSSB protein can destabilize duplex DNA immediately adjacent to both 3′ and 5′ ssDNA extensions may have relevance for a variety of bacterial DNA metabolic processes. The SSB protein may bind at such single-stranded DNA gaps or extensions that are shorter than its site size by using its ability to melt limited regions of adjacent duplex DNA. The presence of such bound SSB protein may facilitate the recruitment of other proteins needed for DNA repair.

ACKNOWLEDGMENT

We thank John R. Battista and his group for assistance in the irradiations of *D. radiodurans* cells needed to carry out the estimation of DrSSB protein concentration in vivo.

REFERENCES

1. Battista, J. R. (1997) Against all odds: The survival strategies of *Deinococcus radiodurans*, *Annu. Rev. Microbiol. 51*, 203−24.
2. Cox, M. M., and Battista, J. R. (2005) *Deinococcus radiodurans*: The consummate survivor, *Nat. Rev. Microbiol. 3*, 882−92.
3. Lohman, T. M., and Ferrari, M. E. (1994) *Escherichia coli* single-stranded DNA-binding protein: Multiple DNA-binding modes and cooperativities, *Annu. Rev. Biochem. 63*, 527−70.
4. Bernstein, D. A., Eggington, J. M., Killoran, M. P., Misic, A. M., Cox, M. M., and Keck, J. L. (2004) Crystal structure of the *Deinococcus radiodurans* single-stranded DNA-binding protein suggests a mechanism for coping with DNA damage, *Proc. Natl. Acad. Sci. U.S.A. 101*, 8575−80.
5. Eggington, J. M., Haruta, N., Wood, E. A., and Cox, M. M. (2004) The single-stranded DNA-binding protein of *Deinococcus radiodurans*, *BMC Microbiol. 4*, 2.
6. Meyer, R. R., and Laine, P. S. (1990) The single-stranded DNA-binding protein of *Escherichia coli*, *Microbiol. Rev. 54*, 342−80.
7. Arana, M. E., Haq, B., Tanguy Le Gac, N., and Boehmer, P. E. (2001) Modulation of the herpes simplex virus type-1 UL9 DNA helicase by its cognate single-strand DNA-binding protein, ICP8, *J. Biol. Chem. 276*, 6840−5.
8. Butland, G., Peregrin-Alvarez, J. M., Li, J., Yang, W., Yang, X., Canadien, V., Starostine, A., Richards, D., Beattie, B., Krogan, N., Davey, M., Parkinson, J., Greenblatt, J., and Emili, A. (2005) Interaction network containing conserved and essential protein complexes in *Escherichia coli*, *Nature 433*, 531−7.
9. Cadman, C. J., and McGlynn, P. (2004) PriA helicase and SSB interact physically and functionally, *Nucleic Acids Res. 32*, 6378−87.
10. Genschel, J., Curth, U., and Urbanke, C. (2000) Interaction of *E. coli* single-stranded DNA binding protein (SSB) with exonuclease I. The carboxy-terminus of SSB is the recognition site for the nuclease, *Biol. Chem. 381*, 183−92.
11. Handa, P., Acharya, N., and Varshney, U. (2001) Chimeras between single-stranded DNA-binding proteins from *Escherichia coli* and *Mycobacterium tuberculosis* reveal that their C-terminal domains interact with uracil DNA glycosylases, *J. Biol. Chem. 276*, 16992−7.
12. Ma, Y., Wang, T., Villemain, J. L., Giedroc, D. P., and Morrical, S. W. (2004) Dual functions of single-stranded DNA-binding protein in helicase loading at the bacteriophage T4 DNA replication fork, *J. Biol. Chem. 279*, 19035−45.
13. McInerney, P., and O'Donnell, M. (2004) Functional uncoupling of twin polymerases: Mechanism of polymerase dissociation from a lagging-strand block, *J. Biol. Chem. 279*, 21543−51.
14. Richard, D. J., Bell, S. D., and White, M. F. (2004) Physical and functional interaction of the archaeal single-stranded DNA-binding protein SSB with RNA polymerase, *Nucleic Acids Res. 32*, 1065−74.
15. Sun, S., and Shamoo, Y. (2003) Biochemical characterization of interactions between DNA polymerase and single-stranded DNA-binding protein in bacteriophage RB69, *J. Biol. Chem. 278*, 3876−81.
16. Witte, G., Urbanke, C., and Curth, U. (2003) DNA polymerase III χ subunit ties single-stranded DNA binding protein to the bacterial replication machinery, *Nucleic Acids Res. 31*, 4434−40.
17. Yuzhakov, A., Kelman, Z., Hurwitz, J., and O'Donnell, M. (1999) Multiple competition reactions for RPA order the assembly of the DNA polymerase δ holoenzyme, *EMBO J. 18*, 6189−99.
18. Yuzhakov, A., Kelman, Z., and O'Donnell, M. (1999) Trading places on DNA: A three-point switch underlies primer handoff from primase to the replicative DNA polymerase, *Cell 96*, 153−63.
19. Dabrowski, S., Olszewski, M., Piatek, R., Brillowska-Dabrowska, A., Konopa, G., and Kur, J. (2002) Identification and characterization of single-stranded-DNA-binding proteins from *Thermus thermophilus* and *Thermus aquaticus*: New arrangement of binding domains, *Microbiology 148*, 3307−15.
20. Witte, G., Urbanke, C., and Curth, U. (2005) Single-stranded DNA-binding protein of *Deinococcus radiodurans*: A biophysical characterization, *Nucleic Acids Res. 33*, 1662−70.
21. Shan, Q., Cox, M. M., and Inman, R. B. (1996) DNA strand exchange promoted by RecA K72R. Two reaction phases with different Mg^{2+} requirements, *J. Biol. Chem. 271*, 5712−24.
22. Lohman, T. M., and Overman, L. B. (1985) Two binding modes in *Escherichia coli* single strand binding protein-single stranded DNA complexes. Modulation by NaCl concentration, *J. Biol. Chem. 260*, 3594−603.
23. Ferrari, M. E., Bujalowski, W., and Lohman, T. M. (1994) Cooperative binding of *Escherichia coli* SSB tetramers to single-stranded DNA in the (SSB)35 binding mode, *J. Mol. Biol. 236*, 106−23.
24. Kowalczykowski, S. C., Lonberg, N., Newport, J. W., and von Hippel, P. H. (1981) Interactions of bacteriophage T4-coded gene 32 protein with nucleic acids. I. Characterization of the binding interactions, *J. Mol. Biol. 145*, 75−104.
25. Wang, J., and Julin, D. A. (2004) DNA helicase activity of the RecD protein from *Deinococcus radiodurans*, *J. Biol. Chem. 279*, 52024−32.

26. Ferrari, M. E., and Lohman, T. M. (1994) Apparent heat capacity change accompanying a nonspecific protein-DNA interaction. *Escherichia coli* SSB tetramer binding to oligodeoxyadenylates, *Biochemistry 33*, 12896−910.
27. Lohman, T. M., and Mascotti, D. P. (1992) Nonspecific ligand-DNA equilibrium binding parameters determined by fluorescence methods, *Methods Enzymol. 212*, 424−58.
28. Zimmerman, J. M., and Battista, J. R. (2005) A ring-like nucleoid is not necessary for radioresistance in the *Deinococcaceae*, *BMC Microbiol. 5*, 17.
29. Maron, P. A., Coeur, C., Pink, C., Clays-Josserand, A., Lensi, R., Richaume, A., and Potier, P. (2003) Use of polyclonal antibodies to detect and quantify the NOR protein of nitrite oxidizers in complex environments, *J. Microbiol. Methods 53*, 87−95.
30. Millipore (2005) *Protein Blotting Handbook*, 5th ed., Millipore Corp., Billerica, MA.
31. Otter, T., King, S. M., and Witman, G. B. (1987) A two-step procedure for efficient electrotransfer of both high-molecular-weight (greater than 400,000) and low-molecular-weight (less than 20,000) proteins, *Anal. Biochem. 162*, 370−7.
32. Harris, D. R., Tanaka, M., Saveliev, S. V., Jolivet, E., Earl, A. M., Cox, M. M., and Battista, J. R. (2004) Preserving genome integrity: The DdrA protein of *Deinococcus radiodurans* R1, *PLoS Biol. 2*, e304.
33. Liu, Y., Zhou, J., Omelchenko, M. V., Beliaev, A. S., Venkateswaran, A., Stair, J., Wu, L., Thompson, D. K., Xu, D., Rogozin, I. B., Gaidamakova, E. K., Zhai, M., Makarova, K. S., Koonin, E. V., and Daly, M. J. (2003) Transcriptome dynamics of *Deinococcus radiodurans* recovering from ionizing radiation, *Proc. Natl. Acad. Sci. U.S.A. 100*, 4191−6.
34. Tanaka, M., Earl, A. M., Howell, H. A., Park, M. J., Eisen, J. A., Peterson, S. N., and Battista, J. R. (2004) Analysis of *Deinococcus radiodurans*'s transcriptional response to ionizing radiation and desiccation reveals novel proteins that contribute to extreme radioresistance, *Genetics 168*, 21−33.
35. Daley, J. M., and Wilson, T. E. (2005) Rejoining of DNA double-strand breaks as a function of overhang length, *Mol. Cell. Biol. 25*, 896−906.
36. Datta, K., Neumann, R. D., and Winters, T. A. (2005) Characterization of complex apurinic/apyrimidinic-site clustering associated with an authentic site-specific radiation-induced DNA double-strand break, *Proc. Natl. Acad. Sci. U.S.A. 102*, 10569−74.
37. Christiansen, C., and Baldwin, R. L. (1977) Catalysis of DNA reassociation by the *Escherichia coli* DNA binding protein: A polyamine-dependent reaction, *J. Mol. Biol. 115*, 441−54.
38. Lohman, T. M., and Bujalowski, W. (1990) *Escherichia coli* single-strand binding protein: Multiple single-stranded DNA binding modes and cooperativities, in *The Biology of Nonspecific DNA-Protein Interactions* (Revzin, A., Ed.) pp 131−70, CRC Press, Boca Raton, FL.
39. Raghunathan, S., Kozlov, A. G., Lohman, T. M., and Waksman, G. (2000) Structure of the DNA binding domain of *E. coli* SSB bound to ssDNA, *Nat. Struct. Biol. 7*, 648−52.
40. Daly, M. J., Gaidamakova, E. K., Matrosova, V. Y., Vasilenko, A., Zhai, M., Venkateswaran, A., Hess, M., Omelchenko, M. V., Kostandarithes, H. M., Makarova, K. S., Wackett, L. P., Fredrickson, J. K., and Ghosal, D. (2004) Accumulation of Mn(II) in *Deinococcus radiodurans* facilitates γ-radiation resistance, *Science 306*, 1025−8.
41. Mikhailov, V. S. (2000) Helix-destabilizing properties of the baculovirus single-stranded DNA-binding protein (LEF-3), *Virology 270*, 180−9.
42. Von Hippel, P. H., and McGhee, J. D. (1972) DNA-protein interactions, *Annu. Rev. Biochem. 41*, 231−300.
43. Alatossava, T., Jutte, H., Kuhn, A., and Kellenberger, E. (1985) Manipulation of intracellular magnesium content in polymyxin B nonapeptide-sensitized *Escherichia coli* by ionophore A23187, *J. Bacteriol. 162*, 413−9.
44. Record, M. T., Jr., Courtenay, E. S., Cayley, D. S., and Guttman, H. J. (1998) Responses of *E. coli* to osmotic stress: Large changes in amounts of cytoplasmic solutes and water, *Trends Biochem. Sci. 23*, 143−8.
45. Leibowitz, P. J., Schwartzberg, L. S., and Bruce, A. K. (1976) The in vivo association of manganese with the chromosome of *Micrococcus radiodurans*, *Photochem. Photobiol. 23*, 45−50.
46. Dove, W. F., and Davidson, N. (1962) Cation effects on the denaturation of DNA, *J. Mol. Biol. 5*, 467−78.
47. Record, M. T., Jr., Lohman, M. L., and De Haseth, P. (1976) Ion effects on ligand-nucleic acid interactions, *J. Mol. Biol. 107*, 145−58.
48. Subirana, J. A., and Soler-Lopez, M. (2003) Cations as hydrogen bond donors: A view of electrostatic interactions in DNA, *Annu. Rev. Biophys. Biomol. Struct. 32*, 27−45.
49. Boehmer, P. E., and Lehman, I. R. (1993) Herpes simplex virus type 1 ICP8: Helix-destabilizing properties, *J. Virol. 67*, 711−5.
50. Monaghan, A., Webster, A., and Hay, R. T. (1994) Adenovirus DNA binding protein: Helix destabilising properties, *Nucleic Acids Res. 22*, 742−8.
51. Zijderveld, D. C., and van der Vliet, P. C. (1994) Helix-destabilizing properties of the adenovirus DNA-binding protein, *J. Virol. 68*, 1158−64.
52. Lusetti, S. L., and Cox, M. M. (2002) The bacterial RecA protein and the recombinational DNA repair of stalled replication forks, *Annu. Rev. Biochem. 71*, 71−100.
53. de Laat, W. L., Appeldoorn, E., Sugasawa, K., Weterings, E., Jaspers, N. G., and Hoeijmakers, J. H. (1998) DNA-binding polarity of human replication protein A positions nucleases in nucleotide excision repair, *Genes Dev. 12*, 2598−609.
54. Georgaki, A., and Hubscher, U. (1993) DNA unwinding by replication protein A is a property of the 70 kDa subunit and is facilitated by phosphorylation of the 32 kDa subunit, *Nucleic Acids Res. 21*, 3659−65.
55. Pestryakov, P. E., Khlimankov, D. Y., Bochkareva, E., Bochkarev, A., and Lavrik, O. I. (2004) Human replication protein A (RPA) binds a primer-template junction in the absence of its major ssDNA-binding domains, *Nucleic Acids Res. 32*, 1894−903.
56. Pestryakov, P. E., Weisshart, K., Schlott, B., Khodyreva, S. N., Kremmer, E., Grosse, F., Lavrik, O. I., and Nasheuer, H. P. (2003) Human replication protein A. The C-terminal RPA70 and the central RPA32 domains are involved in the interactions with the 3′-end of a primer-template DNA, *J. Biol. Chem. 278*, 17515−24.

BI061178M